DYNAMICS OF TUBULAR CYLINDRICAL STRUCTURES IN AXIAL FLOW

Michael P. Païdoussis
Department of Mechanical Engineering, McGill University, Montreal, QC, Canada
e-mail: michael.paidoussis@mcgill.ca

The dynamics of slender cylinders in axial flow subject to conventional boundary conditions is recalled first. This is followed by brief reviews and discussion of new developments in (i) the dynamics of unconventionally supported cylinders, e.g. cylinders free at the upstream end and supported at the downstream one, (ii) the dynamics of cylinders subject to both internal and external flow for applications in oil and gas drilling and production, as well as hydrocarbon storage in salt-mined caverns, and (iii) the peculiar dynamics of very long cylinders, such as acoustic streamers used in underwater oil and gas exploration.

Keywords: Cylinders in axial flow; dynamics; static divergence; single- and coupled-mode flutter; unconventionally supported cylinders; cylinders with both internal and external flow; very long cylinders.

1. DYNAMICS OF CYLINDERS IN AXIAL FLOW

Consider a cylinder, modelled as a beam, in axial flow. At low flow velocities, the cylinder is subject to flow-induced damping. At higher flow velocities, however, it may become subject to static and/or dynamic fluidelastic instabilities.

Let the cross-sectional area of the cylinder be A, its length L, diameter D, mass per unit length m, and flexural rigidity EI; let also the mean axial flow velocity be U. For a horizontal system, neglecting pressurization and gravity effects as well as dissipative forces, the simplest form of the equation of motion is

$$EI\frac{\partial^4 y}{\partial x^4} + MU^2\frac{\partial^2 y}{\partial x^2} + 2MU\frac{\partial^2 y}{\partial x \partial t} + \frac{1}{2}\rho DU^2 C_T(L-x)\frac{\partial^2 y}{\partial x^2} + \rho D^2 U^2 C_b\frac{\partial^2 y}{\partial x^2} + \frac{1}{2}\rho DUC_N\left(\frac{\partial y}{\partial t} + U\frac{\partial y}{\partial x}\right) + \frac{1}{2}\rho DC_D\frac{\partial y}{\partial t} + (M+m)\frac{\partial^2 y}{\partial t^2} = 0, \tag{1}$$

where $M = \rho A$ is the virtual or added mass per unit length for lateral motions in unconfined flow, ρ being the fluid density. C_N and C_T are the coefficients of the viscous forces acting on the cylinder in the normal and longitudinal direction, respectively, and C_D is the lateral force coefficient for zero axial flow; C_b is the base drag coefficient in case of a free end. The form above supposes that the downstream end can slide axially or is entirely free; more generally, $L-x$ above must be replaced by $\left[(1-\frac{1}{2}\delta)L - x\right]$ and C_b by $(1-\delta)C_b$, where $\delta = 0$ if the downstream end is free to slide axially or totally free, and $\delta = 1$ if the supports are fixed and do not allow any extension.

Comparing equation (1) to equation (A.1) for a cylinder or pipe with internal flow, we note that, apart from the terms associated with viscous forces, there is complete correspondence in the first, second and third terms, as well as the last one. Here, however, M is not a physical mass, but an equivalent mass of the external fluid flow according to the slender body approximation.

If the cylinder is subjected to an externally applied tension $\overline{T}$ and pressurization $\overline{p}$, then a term equal to $-\left\{\delta\left[\overline{T} + (1-2\nu)\overline{p}A\right](\partial^2 y/\partial x^2)\right\}$ would have to be added in the equation of motion , where ν is the Poisson ratio. Also, if the cylinder is vertical instead of horizontal, gravity and hydrostatic effects have to be taken into account.

Moreover, if the flow past the cylinder is laterally confined by proximity to the flow-containing channel or by the presence of adjacent structures, the added mass M is no longer equal to ρA but to $\chi\rho A$, where $\chi = \left[(D_{ch}^2 + D^2)/(D_{ch}^2 - D^2)\right] > 1$, in which D_{ch} is the diameter of the flow channel; for unconfined flow, $D_{ch} \to \infty$ and $\chi = 1$.

Taking these effects into account [refer to Païdoussis[1),2)]] and now considering a vertical geometry with the cylinder hanging in downward flow, the nondimensional version of the equation of motion may be written as

$$\frac{\partial^4\eta}{\partial\xi^4} + \left\{\chi u^2 - \delta\left[\Gamma + (1-2\nu)\Pi\right] - \left[\tfrac{1}{2}\varepsilon\, c_T u^2(1+h) + \gamma\right]\left[(1-\tfrac{1}{2}\delta) - \xi\right]\right.$$

$$\left. - \tfrac{1}{2}(1-\delta)c_b\, u^2\right\}\frac{\partial^2\eta}{\partial\xi^2} + 2\,\chi\beta^{1/2}u\frac{\partial^2\eta}{\partial\xi\partial\tau} + \left[\tfrac{1}{2}\varepsilon\, c_N u^2(1+h) + \gamma\right]\frac{\partial\eta}{\partial\xi}$$

$$+ \left[\tfrac{1}{2}\varepsilon\, c_N\,\beta^{1/2}\,u + \tfrac{1}{2}\varepsilon\, c\,\beta^{1/2}\right]\frac{\partial\eta}{\partial\tau} + \left[1 + (\chi-1)\beta\right]\frac{\partial^2\eta}{\partial\tau^2} = 0, \tag{2}$$

where

$$\xi = x/L, \qquad \eta = y/L, \qquad \tau = \{EI/(m+\rho A)\}^{1/2}\; t/L^2 \tag{3}$$

and

$$\beta = \frac{\rho A}{\rho A + m}\,, \quad \gamma = \frac{(m-\rho A)g\,L^3}{EI}\,, \quad \Gamma = \frac{\overline{T}L^2}{EI}\,,$$

$$\varepsilon = \frac{L}{D}\,, \quad u = \left(\frac{\rho A}{EI}\right)^{1/2} U\,L\,, \quad \Pi = \frac{\overline{p}A\,L^2}{EI}\,, \quad h = \frac{D}{D_h}\,, \tag{4}$$

$$c_N = \frac{4}{\pi}C_N\,, \quad c_T = \frac{4}{\pi}C_T\,, \quad c_b = \frac{4}{\pi}C_b\,, \quad c = \frac{4}{\pi}\left(\frac{\rho A}{EI}\right)^{1/2} L\,C_D\,.$$

The approximation $c_N = c_T = c_f$ is sometimes used, as in the calculations for some of the figures to be discussed next.

Additional parameters need to be introduced for cantilevered cylinders, presumed to be terminated by an ogival end-piece, notably f which is a measure of how well streamlined the free end is. The simplest free-end boundary conditions are that at $\xi = 1$ the bending moment is zero and the shear force is

$$\frac{\partial^3\eta}{\partial\xi^3} + \chi f\, u^2\frac{\partial\eta}{\partial\xi} + \chi f\,\beta^{1/2}\,u\frac{\partial\eta}{\partial\tau} - \{1 + (\chi f - 1)\beta\}\,\chi_e\frac{\partial^2\eta}{\partial\tau^2} = \frac{\partial^2\eta}{\partial\xi^2} = 0\,, \tag{5}$$

in which $f \to 1$ for a well-streamlined end, and $f \to 0$ for a blunt one; $\chi_e = (1/AL)\int_{L-l}^{L} A(x)\mathrm{d}x$, l being the length of the end-piece.

In this paper, the dynamics is discussed with the aid of Argand diagrams of the dimensionless complex eigenfrequencies of the system, ω_j, as a function of the dimensionless axial flow velocity, u. A typical such diagram for a pinned-pinned cylinder in axial flow is shown in Figure 1. The imaginary components of the first- and second-mode eigenfrequencies, $\mathscr{I}m(\omega_j)$, $j = 1$ and 2, are plotted versus the real parts, $\mathscr{R}e(\omega_j)$, as a function of u. Here,

$$\omega_j = [(\rho A + m)/EI]^{1/2}\,\Omega_j L^2, \tag{6}$$

and Ω_j the jth radian eigenfrequency; u is defined in (4).

Displacements of the cylinder in the jth mode are expressed as $\eta_j(\xi,\tau) = F(\xi)\exp(\mathrm{i}\omega_j\tau)$, where $\xi = x/L$ and $\omega_j = \mathscr{R}e(\omega_j) + \mathrm{i}\mathscr{I}m(\omega_j)$; τ is the dimensionless time. Thus, $\eta(\xi,\tau) \propto \exp[-\mathscr{I}m(\omega_j)]\exp[i\mathscr{R}e(\omega_j)\tau]$. If $\mathscr{I}m(\omega_j) > 0$, motions are damped, whereas if $\mathscr{I}m(\omega_j) < 0$ they are amplified. In the latter case, if $\mathscr{R}e(\omega_j) \neq 0$, the amplified motions are oscillatory, and hence the instability is termed *flutter*; if $\mathscr{R}e(\omega_j) = 0$, we have nonoscillatory amplified motion, i.e. a *static divergence* — or simply *divergence*, for short.

Thus, in Figure 1, oscillations in the first mode are damped for $u < \pi$ approximately. For $u > 3.1406, \mathscr{R}e(\omega_1) = 0$ is reached, and the locus of the first mode bifurcates on the $\mathscr{I}m(\omega)$-axis; one branch crosses the origin at slightly higher u, say $u = u_{cd}$. Thereafter, $\mathscr{R}e(\omega_1) = 0$, and $\mathscr{I}m(\omega_1) < 0$ for that branch of the solution, indicating that a static divergence has occurred at u_{cd}.

At higher u, the first-mode locus which had split into two, as shown in the diagram on the left of the figure, recombines on the $\mathscr{I}m(\omega)$-axis and then leaves it, such that $\mathscr{I}m(\omega_1) < 0$ while $\mathscr{R}e(\omega_1) > 0$,

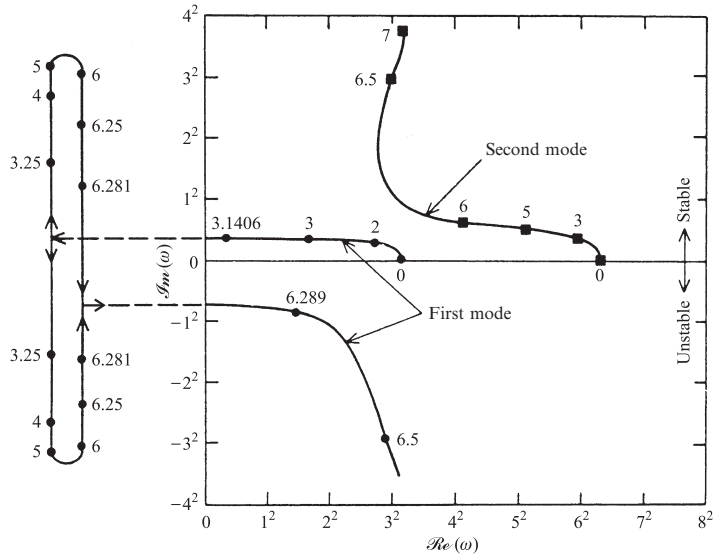

Figure 1: Argand diagram of complex frequencies, ω, of the lowest two modes of a pinned-pinned cylinder in unconfined axial flow, as functions of u for $\beta = 0.48$, $\varepsilon\, c_f = 0.25$ ($c_f = c_T = c_N$), $\delta = \chi = 1$, $c = h = \gamma = \Gamma = 0$; Ref [23].

indicating amplified oscillation (flutter) at a value of u a little higher than $u \simeq 6.281$.* The second-mode locus is always stable in this case, indicating damped oscillation in that mode throughout.

The flutter in Figure 1, which arises from a statically unstable state, is nowadays commonly referred to as a *Païdoussis coupled-mode flutter*, as originally christened by Done & Simpson[3),4)], in contradistinction to classical coupled-mode flutter.[5),6)]

The dynamics of a cantilevered system is illustrated in Figure 2. Here it is seen that the system loses stability by static divergence in its first mode at a value of u a little higher than $u = 2$; it then regains stability in that mode at $u \simeq 5$. For $u \simeq 5.2$, however, stability is lost in the second mode by single-mode flutter via a Hopf bifurcation. Stability is regained in that mode at $u \simeq 8.6$, but meanwhile flutter in the third mode has occurred at $u \simeq 8.25$.

Changing the system parameters, e.g. β or εc_f, alters the dynamics, but the qualitative behaviour generally remains the same. In the case of a cantilevered cylinder, two parameters have a profound effect on the dynamics: f, the free-end streamlining parameter ($f \to 1$ for a well-streamlined free end, and $f \to 0$ for a blunt end), and c_b, a form drag coefficient at the free end. For a sufficiently blunt end ($f \to 0, c_b > 0$) a cantilevered cylinder remains stable, no matter how high u becomes.

It is of considerable interest that for systems subject to a sequence of instabilities as predicted by linear analysis and as shown in Figures 1 and 2, the nonlinear dynamics is not radically different; i.e. the second and higher instabilities predicted by linear theory actually materialize in the nonlinear realm, as they do in the experiments, though the sequence of the bifurcations involved may not be quite the same. In this regard, the routes to instability and the dynamics are quite different from that of the kindred system of a pipe conveying fluid[4),5)].

The behaviour of tapered cylinders in axial flow may also be quite different from that just described, because the boundary layer around the cylinder can become quite thick, thus creating an 'insulating effect' *vis-à-vis* the mean flow.

*Although this flutter is generated by coalescence of branches of the same mode, we still call it a *coupled-mode flutter* — as would be the normal notation if the coalescing branches belonged to two different modes.

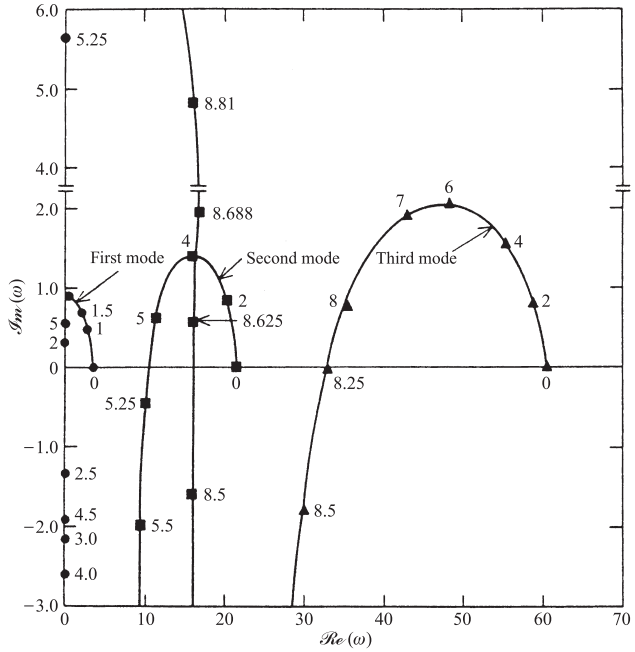

Figure 2: Argand diagram of the complex frequencies, ω, of the lowest three modes of a solitary cantilevered cylinder with a tapered free end in unconfined axial flow, as functions of u, for $\beta = 0.5$, $\varepsilon c_f = 1$, $\delta = 0$, $\chi = 1$, $f = 0.8$, $\chi_e = 0.01$, $c_b = \gamma = 0$; Ref [23].

2. UNCONVENTIONALLY SUPPORTED CYLINDERS IN AXIAL FLOW

The dynamics of 'aspirating cantilevered pipes', i.e. with the flow entering at the free end and exiting at the clamped end, was first studied by Païdoussis in the 1960s as a curiosity and then in 1985 in a simplistic, as it turned out in retrospect, analysis related to ocean mining applications. Later, a number of more elaborate models by Kuiper & Metrikine and Païdoussis *et al.* predicted that the system is unstable either at very low (infinitesimal in the absence of dissipation) flow velocities, or never, with the pendulum of predictions swinging to and fro[1]. The latest is that, for high enough flow velocities, a very weak form of flutter may arise, depending on the fine details of the flow at inlet; refer to Giacobbi *et al.*[7] and section 4.3 of Païdoussis[5].

In the process, this 'reverse flow' problem was related to another, namely that of the reverse (aspirating) sprinkler which has exercised the Physics community from the time of Richard Feynman on, with the same reverses of opinion, as to whether it would rotate or not, and in what sense, as for the potential flutter of the aspirating pipe; refer to Jenkins[8].

Indeed, the study of fluid-structure interactions involving 'reverse flow' has become fashionable. Rinaldi & Païdoussis[9] studied the dynamics of 'free-clamped' cylinders in axial flow; i.e. with the upstream end free and the downstream one clamped, both experimentally and theoretically. For relatively low flow velocities ($U \simeq 5$ m/s, $u \simeq 0.36$), flutter-like oscillatory motions of very small amplitude $A_{\rm rms}$ were observed, such that $A_{\rm rms}/D \sim \mathcal{O}(10^{-3})$, of first-mode frequency and cylinder shape. The oscillation was quite unsteady, with maximum amplitudes 2.5 times the r.m.s. values, similarly to observations for aspirating pipes. Beyond a certain flow velocity, the oscillation amplitude decreased, while a steady bow in the pipe developed and grew, following the classical route to divergence. Thus the system displayed flutter-like oscillations at low flow velocities, and divergence at higher flow velocities. The effect of the upstream-end shape was surprisingly weak.

The flutter-like motions occurred at $u = 0.3 - 0.4$, which is consistent with the predicted behaviour (very small, marginally positive $\mathscr{I}m(\omega_1)$) in Figure 3. However, the discrepancy between the experimental critical flow velocity for divergence, $u_{cd} \simeq 1.1 - 1.7$, and the theoretical $u_{cd} > 2.4$ is rather larger than

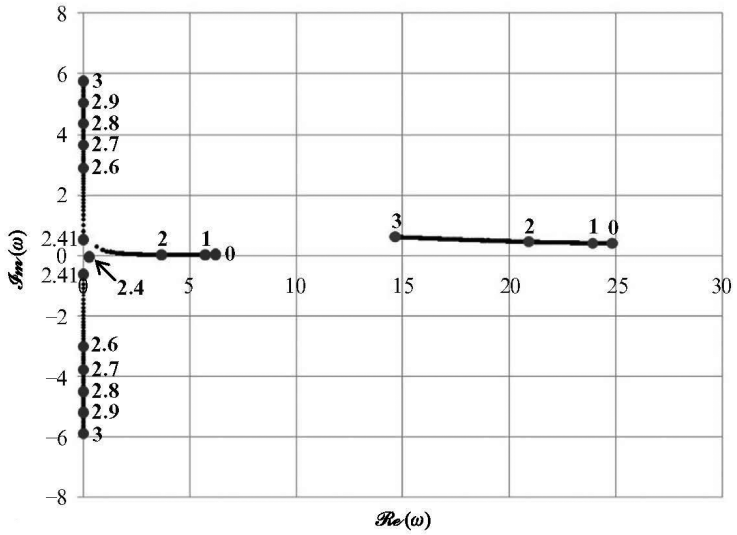

Figure 3: Argand diagram of the lowest two complex eigenfrequencies of a free-clamped cylinder in axial flow for $f = 0.80$ and $c_b = 0.60$, as functions of u; $\beta = 1.14 \times 10^{-3}, \gamma = 17.6, \varepsilon = 25.3, h = 0.455, \chi = 1.22, \chi_e = 0.00792$, $c_N = 0.010, c_T = 0.0125$, and dissipative coefficients $\overline{\alpha}^* = 0.0003, \overline{\mu}^* = 0.0358$; Ref [9].

what could comfortably be attributed to the effect of imperfections; rather, suggesting imperfections in the theory!

The dynamics of pinned-free cylinders was long considered to be not particularly interesting, because the system was thought to be quite similar to a cantilevered one. The problem was re-studied recently by Kheiri & Païdoussis[10], considering a flexibly supported cylinder, as shown in Figure 4, with varying stiffnesses at the support. The pinned-free system was simulated by taking a large value for the transla-

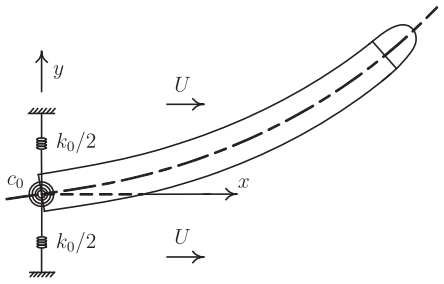

Figure 4: A flexible cylinder subjected to axial flow and supported only at the upstream end by a translational and a rotational spring of stiffnesses k_0 and c_0, respectively.

tional spring stiffness k_0 and zero for the rotational spring stiffness c_0. It was found that the cylinder is unstable from essentially zero flow velocity, the instability being in the form of stationary yawing, as seen in Figure 5; here $\varepsilon^* = \frac{1}{2}\varepsilon c_f$. At higher flow velocities, static/dynamic instabilities in the first and higher modes of the system may occur. It was also found that, by increasing the length of the cylinder while keeping all other parameters constant, the critical flow velocities for various instabilities asymptotically approach constant values; in other words, increasing the length of the cylinder beyond a certain value affects the stability of the system only weakly. Moreover, it was shown numerically and confirmed analytically that there is a limiting value for the length of the cylinder, dependent only on the shape of the tapering end, below which a zero-flow instability may not occur.

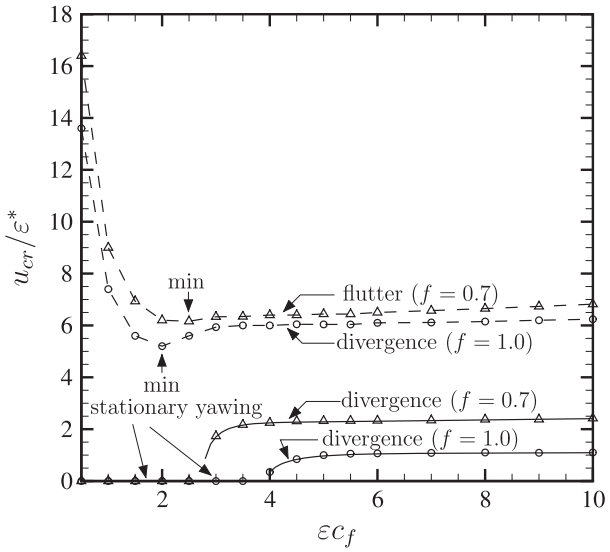

Figure 5: Variation of the critical flow velocity $u_{\rm cr}/\varepsilon^*$, where $\varepsilon^* = \frac{1}{2}\varepsilon c_f$, for static and dynamic instability of a flexible neutrally buoyant (i.e. $\beta = 0.5$) pinned-free cylinder as a function of $\varepsilon c_f (\varepsilon c_f = \varepsilon c_N = \varepsilon c_T)$, in the case of $c_b = 1 - f$; Ref [10].

Additional insights into the dynamics is afforded from consideration of the related problem of a pipe conveying fluid, spring-supported at the upstream end by a translational and a rotational spring; refer to Kheiri *et al.*[11]. It is found that there are ranges in which the critical flow velocity does not change with varying either of the spring stiffnesses. It is also shown that, as the stiffnesses are reduced to low values, the system behaviour approaches that of a free-free pipe: the critical flow velocity is diminished and finally approaches zero.

3. CYLINDERS WITH BOTH INTERNAL AND EXTERNAL FLOW

The dynamics of this system was first studied by Cesari & Curioni[12] and Hannoyer & Paidoussis[13] for its own sake and for applications in axial-flow heat exchangers. The two flows (the fluids and flow velocities) are independent of each other. Later studies were motivated by applications to the drill-string system used in oil and gas drilling pipes; in this case, the internal flow in a vertical pipe, after exiting the drill-bit at the bottom, reverses direction and carries the drilled-out debris upward around the drill-pipe; thus, the internal and external flows are related. This system was first studied by Luu[14] and Païdoussis, Luu & Prabhakar[15].

Argand diagrams for a realistic large-scale drill-string system ($L = 1000$ m) and a bench-top system ($L = 0.443$ m) display qualitatively similar dynamics. Here the dimensionless flow velocities of the internal and external flows, u_i and u_o respectively, are related, depending on $\alpha = D_i/D_o$ and $\alpha_{ch} = D_{ch}/D_o$, where D_i and D_o are the inside and outside diameters of the pipe, and D_{ch} is the diameter of the drilled-out channel. In this case we define two dimensionless flow velocities:

$$u_i = (\rho A_i/EI)^{1/2} U_i L \quad \text{and} \quad u_o = (\rho A_o/EI)^{1/2} U_o L, \tag{7}$$

where A_i is the cross-sectional flow area of the internal flow, U_i the internal flow velocity, and u_o is the same as u in equations (4) with $A \equiv A_o$ and $U \equiv U_o$.

For a wide channel ($\alpha_{ch} = 20$), the dynamics is controlled by the internal flow, as u_i is three orders of magnitude larger than u_o. For small enough u_i, the effect of flow is stabilizing, but for higher u_i it becomes destabilizing (in this case at $u_i \simeq 100$). Similar behaviour is obtained for $\alpha_{ch} = 2$, even though in this case $u_o = 0.3u_i$. For $\alpha_{ch} = 1.1$, however, where $u_o = 4.28u_i$, the external flow plays the dominant role, destabilizing the system and precipitating flutter at $u_i = 0.96$.

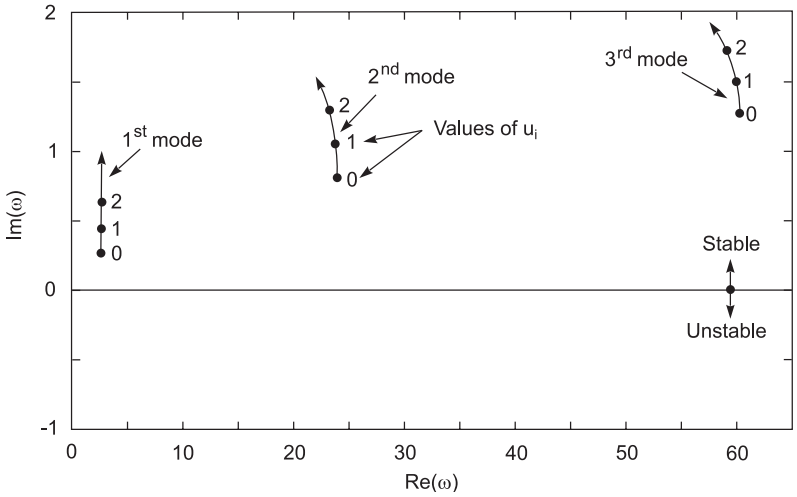

Figure 6: Argand diagram of the complex dimensionless eigenfrequencies of the bench-top-size drill-string-like system, ω_i, $i = 1, 2, 3$ as a function of the dimensionless flow velocity u_i for $\alpha_{ch} = 2.0$.

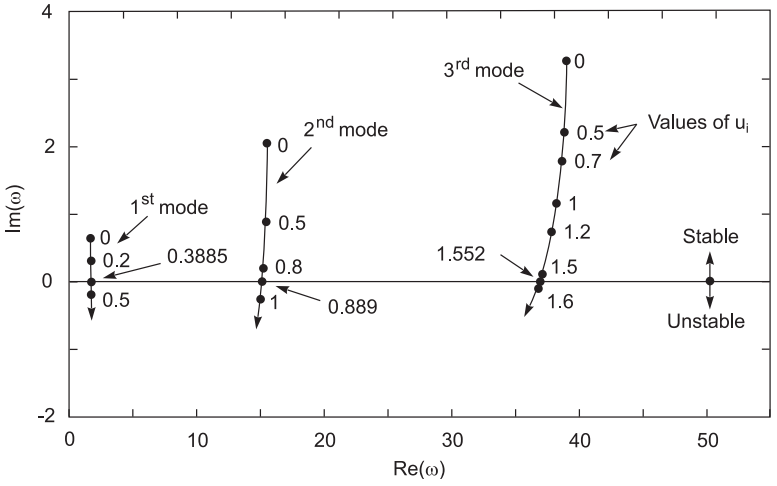

Figure 7: Argand diagram of the complex dimensionless eigenfrequencies of the bench-top-size drill-string-like system, ω_i, $i = 1, 2, 3$ as a function of the dimensionless flow velocity u_i for $\alpha_{ch} = 1.2$.

Similar behaviour is obtained for the bench-top system. As seen in Figure 6 for $\alpha_{ch} = 2.0$, the system is stabilized with increasing flow, as indicated by the increasing positive $\mathscr{I}m(\omega)$ in all the three modes shown. However, for large enough u_i the effect of flow becomes destabilizing; the loci of the second and third modes begin to bend, a preamble to the locus eventually crossing to $\mathscr{I}m(\omega) < 0$ (cf. Figure 2). In this case, the critical flow velocity is $u_{ic} = 6.8$ (not shown).

In Figure 7, on the other hand, where $\alpha_{ch} = 1.2$, the effect of the flow is destabilizing for all u_i. The system loses stability by flutter in the first mode at $u_i \simeq 0.39$. Thus, for large α_{ch} the dynamics is controlled by the internal flow, whereas for small enough α_{ch} it is the external flow which determines stability.

It should finally be remarked that the dimensionless critical flow velocities, u_{ic}, for both the large-scale and bench-top systems are similar, despite large differences in the parameters, particularly L, because the dimensional critical flow velocities for the longer system are proportionately smaller. Thus u_i is a successful scaling parameter.

Further work on this topic has recently been done, related to yet another application: the dynamics of the kilometer long pipe-strings used in salt-mining applications (Ratigan[16]; Moditis *et al.*[17]; Païdoussis[2]) for storing and later retrieving hydrocarbons in solution-mined caverns. Pumping fresh water into underground salt deposits dissolves the salt, generating brine-filled caverns. If the brine is pumped out, there remains a cavern which may be used for storage of liquid or gaseous hydrocarbons. In this case the pipe-string is partly surrounded by a cylindrical tube, creating an annular region. Brine may be pumped into the cavern via the central pipe, forcing the stored hydrocarbon out through the annulus, or *vice versa*. The dynamics is both intricate and quite interesting.

4. VERY LONG CYLINDERS AND STRINGS IN AXIAL FLOW

If the cylinder is sufficiently long and slender, flow-induced tension effects become very important, while the flexural rigidity loses its dominance as the principal restoring force. Thus, the cylinder may be modelled as a taught string, rather than a beam, which also results in a mathematically simpler system.

Here the reader is encouraged to refer to the Doaré & de Langre[18] study of very long hanging pipes conveying fluid, showing the existence of asymptotic regimes in the dynamics, a paradigm for understanding the behaviour of long systems subjected to nonconservative forces.

Towed arrays of hydrophones housed in very long, neutrally buoyant hollow cylinders are the premier example making such systems of practical, as well as academic, interest. In some cases, the existence of a towrope is neglected, and the system is modelled as a cylindrical string supported at its upstream end and free downstream. The dynamics of this latter system is discussed here, while that of towed systems in chapter 4 of Païdoussis[2].

Several analytical studies on the dynamics of this system have been published, unfortunately some based on the equations of motion in Païdoussis[19], containing an error in the viscous forces, which becomes significant for long cylinders, and in other papers with other errors, e.g. Ortloff & Ives[20].

An important study on this system has been done by Triantafyllou & Chryssostomidis[21] with the corrected equations of motion[22),23] in a very elegant analysis, resulting in a remarkably simple stability diagram. The flexural forces are neglected, and tension becomes the main restoring force. The nondimensional equation of motion is

$$[1-p-\varepsilon^*(1-\xi)]\,\frac{\partial^2\eta}{\partial\xi^2}+2\frac{\partial^2\eta}{\partial\xi\partial\tau}+\varepsilon^*\left(\frac{\partial\eta}{\partial\tau}+\frac{\partial\eta}{\partial\xi}\right)+(1+\mu)\frac{\partial^2\eta}{\partial\tau^2}=0\,, \tag{8}$$

subject to boundary conditions

$$\eta(0,\tau)=0, \qquad [(p-f)(\partial\eta/\partial\xi)-f(\partial\eta/\partial\tau)]_{\xi=1}=0\,, \tag{9}$$

where

$$\xi=\frac{x}{L}, \quad \eta=\frac{y}{L}, \quad \tau=\left(\frac{U}{L}\right)t, \quad p=\frac{T_0}{MU^2}, \quad \varepsilon^*=\frac{1}{2}\varepsilon c_f \quad \text{and} \quad \mu=\frac{m}{M}=\frac{1-\beta}{\beta}; \tag{10}$$

here m is the mass of the cylinder and M the virtual (added) mass per unit length, f is a streamlining parameter, as in equation (5), such that $f\to 1$ for a well-streamlined end and $f\to 0$ for a blunt one, T_0 is the free-end tension as in Figure 8, e.g. due to a drogue, but constant rather than flow-velocity dependent.

The stability diagram is shown in Figure 9. Thus, for $\varepsilon^* > 1$ the system is predicted to be unconditionally stable. In the dimensional form of equation (8), the first term is $\left[MU^2-T_0-\frac{1}{2}\rho DU^2C_f(L-x)\right](\partial^2y/\partial x^2)$. Hence, in the range $1-\varepsilon^* < p < 1$ the total tension, $T(x)=T_0+\frac{1}{2}\rho DU^2C_f(L-x)$, becomes equal to MU^2 somewhere along the long string. From thereon there is no tensile restoring force,† and the neglected flexural forces, even if vanishingly small, become important and may have a destabilizing effect on the string.

The stability analysis leading to Figure 9 explicitly presumes the instability to be flutter, since static divergence for a string is not possible, as it would imply the existence of negative tension (compression)

†No self-respecting string can exist without tension, for it is then indistinguishable from a limp strand of overcooked spaghetti.

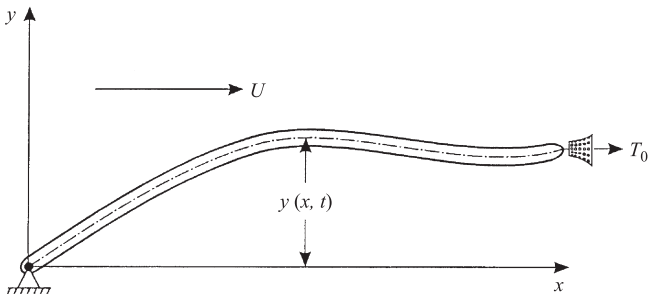

Figure 8: The pinned-free cylinder in axial flow considered by Triantafyllou & Chryssostomidis[21], with a drogue added which generates a tension T_0 at the free end.

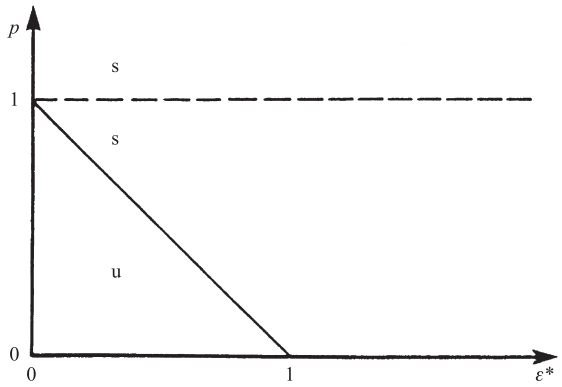

Figure 9: Stability diagram for a pinned-free cylinder in axial flow in terms of the modified slenderness parameter ε^* and the tension parameter p. Stable regions are denoted by s, and the unstable one by u; Ref [21].

over some portion of the string. It is therefore necessary to take into account the flexural restoring forces even for long cylinders, as done by de Langre *et al.*[24].

Placing the origin for $\xi = x/L$ at the downstream end of the cylinder, the analysis is conducted by means of a slightly different form of the equation of motion,

$$\frac{\partial^4\eta}{\partial\xi^4} + \frac{\partial}{\partial\xi}\left[u^2\left(1 - \tfrac{1}{2}c_b + \tfrac{1}{2}\varepsilon c_T\xi\right)\frac{\partial\eta}{\partial\xi}\right] + \frac{1}{2}\varepsilon c_T\left(\frac{c_N}{c_T} - 1\right)u^2\frac{\partial\eta}{\partial\xi}$$
$$+ \frac{1}{2}\varepsilon c_T\left(\frac{c_N}{c_T}\right)\beta^{1/2}u\frac{\partial\eta}{\partial\tau} + 2\beta^{1/2}u\frac{\partial^2\eta}{\partial\xi\partial\tau} + \frac{\partial^2\eta}{\partial\tau^2} = 0, \tag{11}$$

and simplified boundary conditions,

$$\eta(-1) = \frac{\partial\eta}{\partial\xi}(-1) = 0,$$
$$\left[\frac{\partial^2\eta}{\partial\xi^2}\right]_{\xi=0} = \left[\frac{\partial^3\eta}{\partial\xi^3} + fu\left(\beta^{1/2}\frac{\partial\eta}{\partial\tau} + u\frac{\partial\eta}{\partial\xi}\right)\right]_{\xi=0} = 0. \tag{12}$$

It is clear that in (11) there generally exists a location $\xi_c = -L_c/L = -(2 - c_b)/\varepsilon c_T$, where the flow-induced tension vanishes; this location is referred to as the *neutral point*. Downstream of that point the cylinder is *in compression*. This at-first-sight surprising statement becomes perfectly understandable by reference to the similar system of a pipe conveying fluid [refer to Appendix A].

The analysis is pursued in terms of the above equations, but also in terms of similar but significantly different ones in which the scaling length is not L but L_c; thus,

$$z = x/L_c, \quad v = (\rho A/EI)^{1/2}UL_c = u/l, \quad l = L/L_c, \tag{13}$$

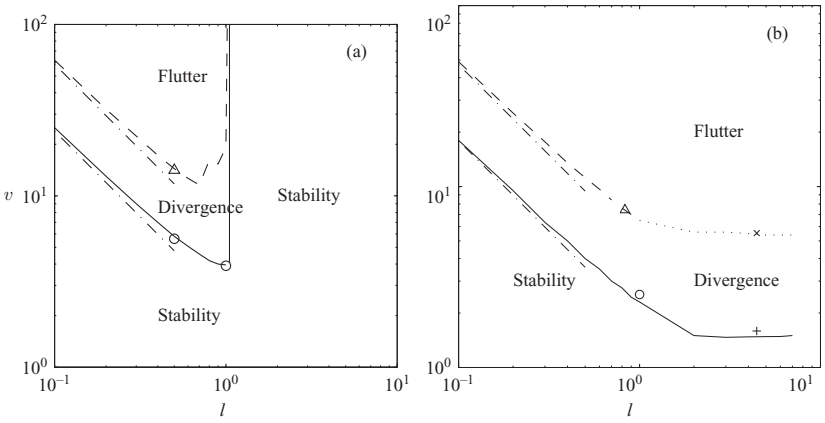

Figure 10: Effect of length on the stability of a cylinder, (a) for a system stable at high enough l, with $f = 0.5$, (b) for a system unstable at high l, with $f = 0.8$: —, critical flow velocity for divergence; $-\ -\ -$, critical value for flutter by Hopf bifurcation; $\cdots$, critical value for Païdoussis-type flutter; $-\cdot-$, critical value for divergence and flutter of short cylinders; $\circ, \triangle$, for cylinders of intermediate length; $\times, +$, for long cylinders; Ref [24].

etc. Numerical results are obtained via the Galerkin method[4),1)] and a finite difference scheme[25)]. Interesting new results are obtained, supplemented by some determined earlier by Semler *et al.*[26)], as shown in Figure 10.

For a fairly blunt end ($f = 0.5$), it is seen in Figure 10(a) that both divergence and flutter cease to exist for $l \geq 1$. In terms of dependence on length, Semler *et al.*[26)] find that divergence occurs at $u = 2.39$ for $\varepsilon c_N = 0$, yielding the asymptotic relation $v = 2.39/l$, which compares well with the Semler *et al.* results. Similarly, $v = 5.87/l$ for flutter, which again gives results consistent with those of Semler *et al.*

For a well-streamlined end, $f = 0.8$, on the other hand, both divergence and flutter persist to $l \simeq 10$ (Figure 10(b)) and beyond, in both cases reaching a plateau for $l \geq 2$ approximately. For small l the flutter is via a Hopf bifurcation, while for $l > 1$ it is of the Païdoussis coupled-mode type.

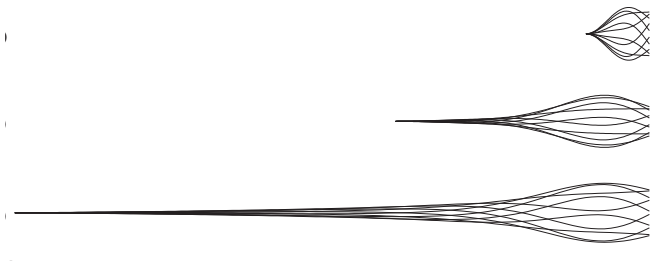

Figure 11: Modal shapes of the flutter modes for $f = 0.8$: and, top to bottom, $l = 0.5, 2$ and 5, respectively; Ref [24].

In Figure 11 we see the shape of the unstable mode for several values of l. The flutter mode shape is evaluated at $v \simeq 1.1 v_c$, neglecting the imaginary component of the frequency (the growth rate) for clarity. These results confirm the existence of limit regimes for long cylinders where both divergence and flutter exist, with the motion confined to a downstream portion of the cylinder, typically of size L_c.

The existence of flutter for very long cylinders contradicts previous predictions of the dynamics by Triantafyllou & Chryssostomidis[21)] and Dowling[27)]. Below, we discuss how this has come about, despite all analyses being free of error.

In the Triantafyllou & Chryssostomidis analysis, the cause of instability is related to the disappearance of tension, i.e. the absence of any stiffness in the system. However, in the de Langre *et al.*[24)] analysis it is shown that the presence of even a small bending rigidity is sufficient to stabilize the system for small enough f. Therefore, the string model is inappropriate for assessing stability of cylinders of small bending stiffness.

The reason why flutter is not predicted in the Dowling analysis is simpler. For long cylinders, flutter is of the Païdoussis type, emanating from a static divergence solution, which we know does exist (Triantafyllou & Cryssostomidis[28]). In the Dowling analysis divergence is excluded, as it implies the existence of negative tension, and thereby so is flutter.

The most important findings of this work are that (i) long cylinders with a streamlined free end are not immune to flutter and (ii) the dynamics of long cylinders may be approximated by that of cylinders of length L_c.

CONCLUSION

The dynamics of tubular cylindrical structures in axial flow has been reviewed briefly in this paper, focusing on new developments, as discussed in Sections 2-4. Several other facets of the system have been explored over the past 10-15 years, but are not discussed in this paper, for example (i) flexible cylinders being extruded or deployed in dense fluid, (ii) self-propelled articulated cylinders modelling trains going through tunnels, pipelines towed underwater for installation farther afield, propulsion of autonomous underwater vehicles and aquatic drones, including a great deal of new work on fish locomotion. The interested reader is referred to chapters 3 and 4 of Païdoussis[2].

APPENDIX A: DYNAMICS OF A PIPE CONVEYING FLUID

As discussed in Païdoussis[4),5)] at length, the simplest form of the equation of motion of a pipe conveying fluid is

$$EI\frac{\partial^4 y}{\partial x^4} + MU^2\frac{\partial^2 y}{\partial x^2} + 2MU\frac{\partial^2 y}{\partial x \partial t} + (M+m)\frac{\partial^2 y}{\partial t^2} = 0, \tag{A.1}$$

where all the symbols have the same meaning as in the main text of this paper, except that M here is the mass of the conveyed fluid per unit length. The first term is the flexural restoring force, the third is the Coriolis force, and the second is the follower compressive force term; cf. the equation of motion of a beam subject to a compressive force P,

$$EI(\partial^4 y/\partial x^4) + P(\partial^2 y/\partial x^2) + m(\partial^2 y/\partial t^2) = 0. \tag{A.2}$$

The viscous frictional terms in (1) do not exist for internal flow.

For a cantilevered cylinder in axial flow, we also have a tension due to traction. As discussed in Section 4, beyond the neutral point, the flow-induced tension vanishes, and the cylinder is under compression. The system loses stability by static divergence, and at higher flow velocities by Païdoussis-type coupled-mode flutter. For a short cylinder, however, flutter can arise via a Hopf bifurcation, as in Figure 2.

ACKNOWLEDGEMENT

Support of this research by the Natural Sciences and Engineering Research Council of Canada (NSERC), the Salt Mining Research Institute (SMRI) and Pipeline Research Council International (PRCI) is gratefully acknowledged.

REFERENCES

1) Païdoussis, M.P.: *Fluid-Structure Interactions: Slender Structures and Axial Flow*, Volume 2. London: Elsevier Academic Press, 2004.

2) Païdoussis, M.P.: *Fluid-Structure Interactions: Slender Structures and Axial Flow*, Volume 2, 2nd edition. London: Elsevier Academic Press, 2016.

3) Done, G.T.S., Simpson, A.: Dynamic stability of certain conservative and non-conservative systems. *I.Mech.E. J. Mech. Eng. Sci.*, Vol. 19, pp. 251-263, 1977.

4) Païdoussis, M.P.: *Fluid-Structure Interactions: Slender Structures and Axial Flow*, Volume 1. London: Academic Press, 1998.

5) Païdoussis, M.P.: *Fluid-Structure Interactions: Slender Structures and Axial Flow*, Volume 1, 2nd edition. London: Elsevier Academic Press, 2014.

6) Païdoussis, M.P., Price, S.J., de Langre, E.: *Fluid-Structure Interactions: Cross-Flow-Induced Instabilities*. Cambridge: Cambridge University Press, 2011.

7) Giacobbi, D.B., Rinaldi, S., Semler, C., Païdoussis, M.P.: The dynamics of a cantilevered pipe aspirating fluid studied by experimental, numerical and analytical methods. *J. Fluids Struct.*, Vol. 30, pp. 73-96, 2012

8) Jenkins, A.: Sprinkler head revisited: momentum, forces and flows in Machian propulsion. *Eur. J. Physics*, Vol. 32, pp. 1213-1226, 2011.

9) Rinaldi, S., Païdoussis, M.P.: Theory and experiments on the dynamics of a free-clamped cylinder in confined axial air-flow. *J. Fluids Struct.* Vol. 28, pp. 167-179, 2012.

10) Kheiri, M., Païdoussis, M.P.: Dynamics and stability of a flexible pinned-free cylinder in axial flow. *J. Fluids Struct.*, Vol. 55, pp. 204-217, 2015.

11) Kheiri, M., Païdoussis, M.P., Amabili, M.: An experimental study of dynamics of towed flexible cylinders. *J. Sound Vib.*, Vol. 348, pp. 149-166, 2015.

12) Cesari, F., Curioni, S.: Buckling instability in tubes subject to internal and external axial fluid flow. In *Proc. 4th Conf. on Dimensioning*, Budapest: Hungarian Academy of Science, pp. 301-311, 1971.

13) Hannoyer, M.J., Païdoussis, M.P.: Instabilities of tubular beams simultaneously subjected to internal and external axial flows. *ASME J. Mech. Design*, Vol. 100, pp. 328-336, 1978.

14) Luu, T.P.: On the dynamics of three systems involving tubular beams conveying fluid. M.Eng. Thesis, Dept. Mech. Eng., McGill University, Montreal, Québec, Canada, 1983.

15) Païdoussis, M.P., Luu, T.P., Prabhakar, S.: Dynamics of a long tubular cantilever conveying fluid downwards, which then flows upwards around the cantilever as a confined annular flow. *J. Fluids Struct.*, Vol. 24, pp. 111-128, 2008.

16) Ratigan, J.: Brine string integrity and model simulation. *Proc. 2nd SMRI Tech. Conf.*, Galveston/ Austin, TX, USA, pp. 273-293, 2008.

17) Moditis, K., Païdoussis, M.P., Ratigan, J.: Dynamics of a partially-confined, discharging, cantilever pipe with reverse external flow, *J. Fluids Struct.*, under review, 2015.

18) Doaré, O., de Langre, E.: The flow-induced instability of long hanging pipes. *Eur. J. Mechanics A/Solids*, Vol. 21, pp. 857-867, 2002.

19) Païdoussis, M.P.: Dynamics of flexible slender cylinders in axial flow. Part 1: theory. Part 2: experiments. *J. Fluid Mech.*, Vol. 26, pp. 717-736 and pp. 737-751, 1966.

20) Ortloff, C.R., Ives, J.: On the dynamic motion of a thin flexible cylinder in a viscous stream. *J. Fluid Mech.*, Vol. 38, pp. 713-720, 1969.

21) Triantafyllou, G.S., Chryssostomidis, C.: Stability of a string in axial flow. *ASME J. Energy Res. Tech.* , Vol. 107, pp. 421-425, 1985.

22) Païdoussis, M.P.: Dynamics of submerged towed cylinders. *Eighth Symp. Naval Hydrodynamics: Hydrodynamics in the Ocean Environment.* U.S. ONR, ARC-179, pp. 981-1016, 1970.

23) Païdoussis, M.P.: Dynamics of cylindrical structures subjected to axial flow. *J. Sound Vib.*, Vol. 29, pp. 365-385, 1973.

24) de Langre, E., Païdoussis, M.P., Doaré, O., Modarres-Sadeghi, Y.: Flutter of long flexible cylinders in axial flow. *J. Fluid Mech.*, Vol. 571, pp. 371-389, 2007.

25) Sugiyama, Y., Kawagoe, H.: Vibration and stability of elastic columns under the combined action of uniformly distributed vertical and tangential forces. *J. Sound Vib.*, Vol. 38, pp. 341-355, 1975.

26) Semler, C., Lopes, J.-L., Augu, N., Païdoussis, M.P.: Linear and nonlinear dynamics of cantilevered cylinders in axial flow. Part 3: Nonlinear dynamics. *J. Fluids Struct.* Vol. 16, pp. 739-759, 2002.

27) Dowling, A.P.: The dynamics of towed flexible cylinders. Part 1: neutrally buoyant elements. *J. Fluid Mech.*, Vol. 187, pp. 507-532, 1988.

28) Triantafyllou, G.S., Chryssostomidis, C.: Analytic determination of the buckling speed of towed slender cylindrical beams. *ASME J. Energy Res. Tech.*, Vol. 106, pp. 246-249, 1984.

Prof. Emeritus

Michael P. Païdoussis(McGill University, Canada)

Michael P. Païdoussis was born in Cyprus in 1935, and was educated in the Greek Schools of Egypt, McGill University and the University of Cambridge, receiving his B.Eng. in Mechanical Sciences (with honours) in 1958 and his Ph.D. (Cantab) in Engineering in 1963. He has been Overseas Fellow at GEC in Britain (1958-60) and Research Officer at Atomic Energy of Canada Ltd (Applied Physics Division, 1963-67) in Chalk River, Canada. He joined the Department of Mechanical Engineering of McGill University in 1967. Promoted to Professor in 1976, he served as Chairman of the Department from 1977 to 1986, and now is the Thomas Workman Professor Emeritus. Since 1960, he has worked on various aspects of fluid-structure interactions and flow-induced vibrations and instabilities. He is the author of “Fluid-Structure Interactions: Slender Structures and Axial Flow”, Vol. 1 (1998, 2nd edition 2014, Academic Press, London), Vol. 2 (2004, Elsevier Academic Press, London), and co-author of "Fluid-Structure Interactions: Cross-Flow-Induced Instabilities", (2011, Cambridge University Press). He has published 215 papers in refereed journals and 136 full papers in refereed conference proceedings. He has received a British Association Medal for High Distinction in Mech. Engineering (1958), the George Stephenson Prize from the Institution of Mechanical Engineers (IMechE) in 1975, the CANCAM Prize in 1995, and the ASME 1999 Fluids Engineering Award. He is Fellow of IMechE, ASME, CSME, the American Academy of Mechanics, the Royal Society of Canada (Academy of Science), and the Canadian Academy of Engineering. He has served as Chairman of Division III of IAHR (1981-87), and has been active in various committees of the Pressure Vessels and Piping, Fluids Engineering and Applied Mechanics Divisions of ASME; he was the ASME Calvin Rice Lecturer for 1992, and was elevated to Life Fellow. He is the founding Editor (1986) of the Journal of Fluids and Structures (Academic Press, now Elsevier).